

Conf-930726--8

Wind Turbine Blade Aerodynamics: the Combined Experiment

Marvin W. Luttges
Mark S. Miller
Michael C. Robinson
Derek E. Shipley
Teresa S. Young

*Prepared for
Windpower '93
July 12-16, 1993
San Francisco, California*



National Renewable Energy Laboratory
1617 Cole Boulevard
Golden, Colorado 80401-3393
A national laboratory of the U.S. Department of Energy
Managed by Midwest Research Institute
for the U.S. Department of Energy
under contract No. DE-AC36-83CH10093

Prepared under Task No. WE418120

August 1994

MASTER *ds*

DISTRIBUTION OF THIS DOCUMENT IS UNLIMITED

NOTICE

This report was prepared as an account of work sponsored by an agency of the United States government. Neither the United States government nor any agency thereof, nor any of their employees, makes any warranty, express or implied, or assumes any legal liability or responsibility for the accuracy, completeness, or usefulness of any information, apparatus, product, or process disclosed, or represents that its use would not infringe privately owned rights. Reference herein to any specific commercial product, process, or service by trade name, trademark, manufacturer, or otherwise does not necessarily constitute or imply its endorsement, recommendation, or favoring by the United States government or any agency thereof. The views and opinions of authors expressed herein do not necessarily state or reflect those of the United States government or any agency thereof.

Available to DOE and DOE contractors from:
Office of Scientific and Technical Information (OSTI)
P.O. Box 62
Oak Ridge, TN 37831
Prices available by calling (615) 576-8401

Available to the public from:
National Technical Information Service (NTIS)
U.S. Department of Commerce
5285 Port Royal Road
Springfield, VA 22161
(703) 487-4650



Printed on paper containing at least 50% wastepaper and 10% postconsumer waste

"WIND TURBINE BLADE AERODYNAMICS: THE COMBINED EXPERIMENT"

M.C. Robinson, M.W. Luttges, M.S. Miller, D.E. Shipley and T.S. Young
Department of Aerospace Engineering Sciences
University of Colorado - Boulder, 80309

ABSTRACT

Data obtained from the National Renewable Energy Laboratory site test of a wind turbine (The Combined Experiment) was analyzed specifically to capture information regarding the aerodynamic loading experienced by such machines. The analysis showed that inflow conditions were extremely variable and that these inflows yielded three different operational regimes. Each regime produces very different aerodynamic loading conditions that must be tolerated by the turbine. The two conditions not predicted from wind tunnel data are being subjected to further analyses to provide new guidelines for both designers and operators.

INTRODUCTION

Horizontal and vertical axis wind turbines operating in the field experience one of the most complex flow environments of any aerodynamic device. Horizontal turbine geometries provide highly three-dimensional flows with strong radial (span wise) pressure and velocity gradients. Highly variable wind conditions can produce major alterations in the inlet flow magnitude and direction. These alterations in the inlet behavior may be further complicated by the addition of other large flow disturbances introduced from turbines operating upwind as is typical in wind farms. This combination of turbine geometry and unsteady inlet flow conditions vary the localized turbine blade velocity field along the span producing, simultaneously, blade operating environments ranging from fully stalled to fully attached flow. The rapidly changing inlet flow conditions can dynamically drive the flow separation and create extremely large, non-linear, transient loading along the blade span. These loads can be experienced throughout the remaining elements of the wind turbine. Overall a major toll can be produced on the wind turbines to shorten the operational life and to produce high maintenance requirements for these machines.

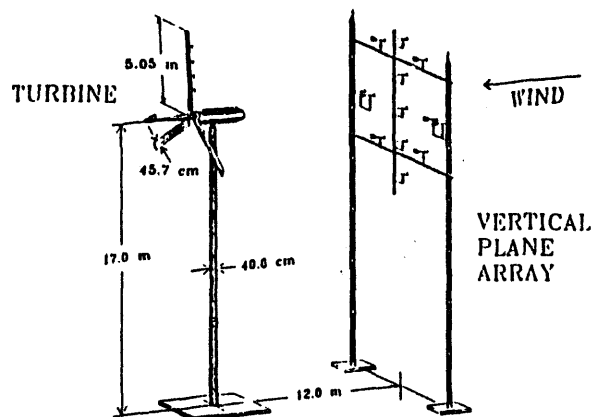


FIGURE 1: VIEW OF THE COMBINED EXPERIMENT TEST SITE INCLUDING THE GRUMMAN WIND STREAM 33 HORIZONTAL AXIS WIND TURBINE AND THE VERTICAL PLANE ARRAY.

NREL's "Combined Experiment" has provided an extensive data set aimed at understanding the aerodynamic responses elicited from turbines operating in the field (Butterfield 1992). This highly instrumented horizontal axis wind turbine (Fig. 1) was used to collect a wide variety of aerodynamic and turbine performance data.

The present investigation focuses on the aerodynamic response of the turbine blade as a consequence of turbine geometry and inlet flow conditions. From the massive data set analysis that has been completed, only a small portion of the unsteady pressure data collected along the span and the correlated inlet flow conditions monitored by the vertical plane array located upstream are reported here.

In order to quantify the unsteady aerodynamic performance of a horizontal wind turbine, it was first necessary to systematically categorize the data by both "steady" and "unsteady" performance indices. Establishing the steady aerodynamic response of the turbine under relatively steady inflow conditions was critical in determining the baseline performance metric for the Combined Experiment Turbine. Using this metric it was possible to cross check the performance against existing wind tunnel data. Then, off-nominal responses or anomalous responses of the turbine to unsteady inlet flow conditions could be carefully identified and quantified. A complete description of the methods used to establish the baseline performance under steady conditions is reported. Only a sample of the unsteady turbine performance reduction is included here, the complete unsteady analysis data will be reported at a later date. Importantly, it has been possible to clearly differentiate the steady from unsteady effects recorded throughout the Combined Experiment test data. Simple, large scale averaging techniques do not reveal these important operational differences and do not clearly identify changes in operational strategies that could minimize some of the undesirable unsteady aerodynamic loading effects on wind turbines operating in the field environment.

METHODS

NREL's Combined Experiment horizontal axis wind turbine is a 10.1 meter diameter, three-bladed machine that rotates at a constant 72 RPM and is capable of producing 20 kW of power. The turbine is supported on a 0.4 meter cylindrical column at a height of 17 meters from the ground to the center of the hub. The blades used were rectangular, untwisted NREL S809 airfoil sections with an 18 in. chord. One of the three blades was completely instrumented with pressure transducers (Fig. 2) at four different span locations. Unsteady pressure data from all transducers were collected simultaneously. The data sample rate (521 Hz, Table 1) was sufficient to capture the dynamic and transient pressure events elicited from time variant inlet flow conditions.

The inlet flow conditions were measured by the vertical plane array located 12 meters upwind of the turbine. The inlet flow magnitude and direction across the turbine diameter was measured using 11 prop-vane and 2 bi-vane anemometers. Eight of the prop-vane anemometers were arranged in a 4 meter radius circle approximately 16 meters above the ground. The remaining anemometers were spaced evenly inside the circle in a vertical line. The two bi-plane anemometers were mounted outside the circle on the horizontal axis. These 13 anemometers permitted a detailed characterization of the inlet flow conditions.

Data was collected over a wide range of nominal operating conditions for the turbine. Each data run consisted of a five minute continuous data collection episode wherein all data were stored on time encoded tape. The turbine blade rotated at a constant 1.2 Hz, thus, 360 consecutive blade rotation cycles are contained in each 5 minute episode. A total of 59 episodes were collected representing 21,000 complete rotation cycles of

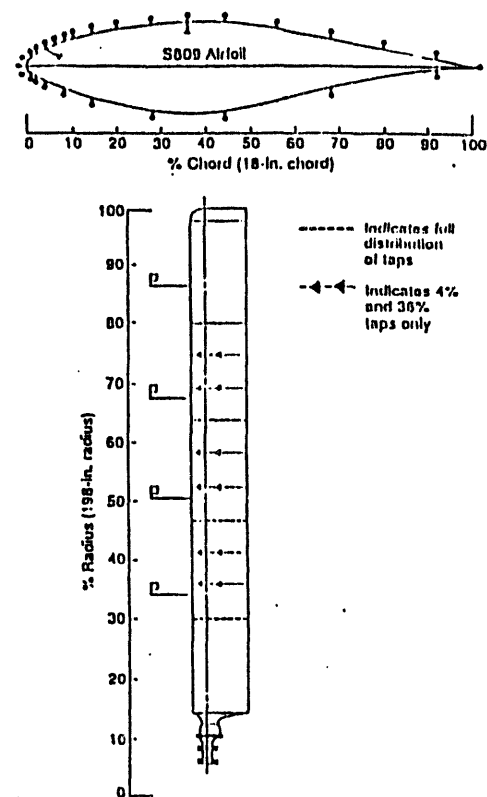


FIGURE 2: ROTOR BLADE CROSS SECTION AND LONGITUDINAL VIEWS SHOWING CHORDWISE PRESSURE TAP DISTRIBUTION AT EACH OF FOUR PRIMARY LOCATIONS: 30%, 47%, 63%, AND 80% SPAN.

the instrumented turbine blade. The total 59 tape data set consists of 9 Gbytes of data and requires 30 optical disks for storage.

ANALYSIS & DISCUSSION

For any airfoil blade the pressure distributions over the chord and span in conjunction with the normal and tangential force distributions obtained from integration of the pressure distributions provide a complete description of the blade aerodynamic response. Previous data reduction approaches (Huyer 1993) had used a cycle averaged, integrated pressure approach to resolve the aerodynamic response at different span locations along the blade. This method inherently assumes the existence of well-behaved data sets exhibiting normal distributions of the critical independent variables (inlet flow velocities and angles). Applying this technique to data without a normalized distribution can average out the transient aerodynamic responses that actually take a toll on machine performance and life.

It was necessary to examine the whole existing data set to determine whether or not there were major excursions of wind velocities and angles that would make averaging techniques relatively useless. In other words, major changes in inflow conditions during testing episodes could change the aerodynamic operating conditions of the airfoils of the Combined Experiment such that no clear indications of the aerodynamics of this wind turbine could be established. Without such information, it would be impossible to envision changes in field operations that might reduce some of the aerodynamic tolls paid by wind turbine machinery.

In order to fully appreciate the baseline performance of horizontal axis wind turbines under steady inflow conditions, it is important to understand the effects that turbine geometry and inlet flow variables have on the turbine blade aerodynamic response (Fig. 3). The local angle of attack is, of course, a major determinant in airfoil aerodynamic performance. At any span location the angle of attack on a rotor airfoil blade is the product of three variables: 1) Inlet flow velocity, 2) blade rotational velocity at that span location, and 3) yaw angle of the turbine disk relative to the inflow. Any change in these variables will alter the local angle of attack and affect the blade aerodynamic response. Rapid changes in these variables alter the angle of attack dynamically and will produce aerodynamic conditions not predictable from common steady angle of attack conditions. Under the right conditions, these rapid changes can produce many effects including dynamic stall where extremely high (up to 10 fold) aerodynamic loads are produced for brief periods of time.

The effects of velocity and span location on the local blade angle of attack for this test geometry are shown in Fig. 4. Increasing the inlet velocity increases the local blade angle of attack. Small

TABLE 1: SUMMARY OF MEASURED DATA CHANNELS GROUPED BY MEASUREMENT LOCATION AND SAMPLING RATE.

Turbine Rotor		Upper Surface		Lower Surface
520 83 Hz Sample Rate				
Pressure Measurement Locations (ESP-32 transducers)				
30% Span		15		10
35 8% Span		2		
41 1% Span		2		
47% Span		18		10
52 2% Span		2		
57 8% Span		2		
63% Span		18		10
68 8% Span		2		
74 4% Span		2		
80% Span		18		10
4 Total Pressure Probes (34%, 50.6%, 67.3%, 86% span)				
Force Measurements				
4 Root Flap Bending				
5 Flap Bending (20%, 40%, 50%, 70%, 90% span)				
3 Edge Bending (0%, 50%, 70% span)				
3 Blade Torque (0%, 20%, 80% span)				
2 Low Speed Shaft Bending				
2 Low Speed Shaft Torque				
Atmospheric Condition				
1 Absolute Pressure Reference				
Miscellaneous Measurements				
4 Angle of Attack (34%, 50.6%, 67.3%, 86%)				
1 Pitch Angle				
Vertical Plane Array (VPA)				
69.44 Hz Sample Rate				
Local MET Tower				
277.78 Hz Sample				
Wind Speed				
11 Prop Vane Anemometers				
2 Bi-Vane Anemometers				
Wind Direction				
1 Prop Vane Anemometer				
2 Bi-Vane Anemometers				
Wind Angle				
2 Bi-Vane Anemometers				
Nacelle & Tower				
277.78 Hz Sample Rate				
Force Measurements				
1 Yaw Moment				
2 Tower Bending				
Miscellaneous Measurements				
1 Low Speed Shaft Azimuth Angle				
1 Yaw Angle				
1 Generator Power				
Far Met Tower				
34.72 Hz Sample Rate				
Wind Speed				
4 Teledyne Cup Anemometers (at heights of 5 m, 10 m, 20 m, 50 m)				
Wind Direction				
4 Teledyne Vane Anemometers (at heights of 5 m, 10 m, 20 m, 50 m)				
Atmospheric Conditions				
2 Air Temperature (at heights of 5 m and 50 m)				
1 Barometric Pressure				

variations in velocity (appx. 5 m/s) can change the blade angle from attached flow (15 deg) to a fully separated (20 deg) flow condition. The effect of the span rotational velocity is also apparent in this Figure. At any velocity, inboard span locations (30%) have a smaller rotational velocity component and angle of attack is more dependent on the incoming flow velocities. Moving outward from the rotor hub increases the span location and increases the velocity component in the plane of the turbine rotation. Thus, the wind velocity contribution to angles of attack is reduced. Accordingly, the velocity vector sum decreases the angle of attack at span locations near the rotor blade tip (80%).

The relative orientation of the turbine to the inlet velocity vector defines the turbine yaw angle. When the yaw angle is not equal to zero degrees (wind perpendicular to the rotation plane), the total velocity relative to the local blade has a strong periodic component that varies from when the blade is rotating into the wind to instances where the blade is moving away from it. The resulting angle of attack is, therefore, also periodic. The magnitude of the angle variation depends on the inlet velocity, yaw angle and

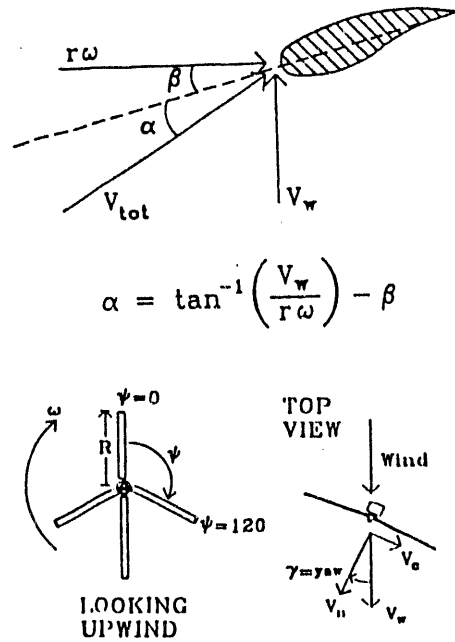


FIGURE 3: GEOMETRICAL RELATIONSHIPS BETWEEN INFLOW VARIABLES AND A DOWNWIND HORIZONTAL AXIS WIND TURBINE. THE TOP FIGURE DEFINES ANGLE OF ATTACK AND THE FIGURES ON THE BOTTOM DEPICT AZIMUTH ANGLE AND YAW ANGLE.

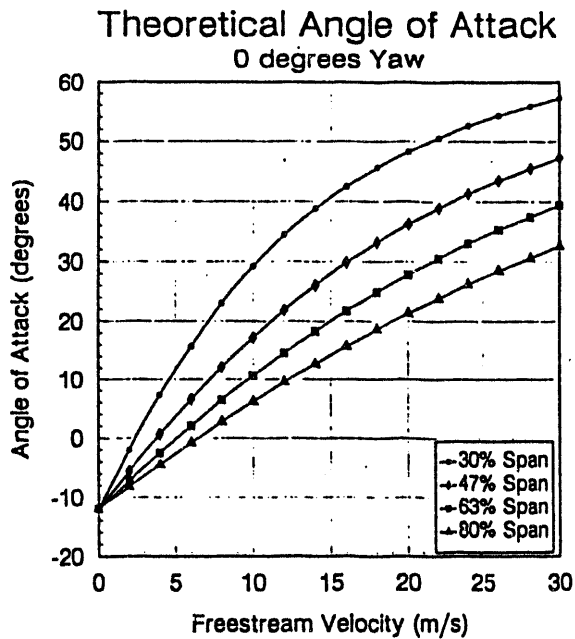


FIGURE 4: THEORETICAL ANGLE OF ATTACK BASED ON FREESTREAM VELOCITY AT ZERO DEGREES YAW FOR 30%, 47%, 63%, AND 80% SPAN.

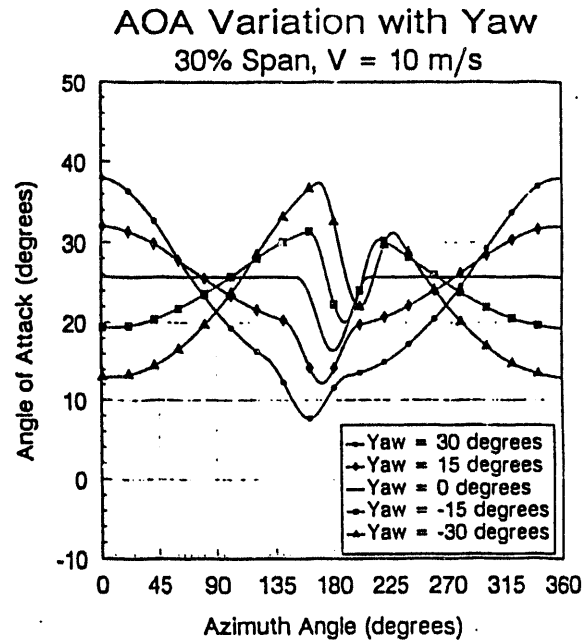


FIGURE 5: VARIATION OF ANGLE OF ATTACK OVER A ROTATIONAL CYCLE AT VARIOUS YAW ANGLES FOR 30% SPAN. THE EFFECT OF PASSAGE THROUGH THE TOWER SHADOW IS ALSO ILLUSTRATED.

span location. Fig. 5 shows the angle of attack change for various yaw angles at 30% span and 10 m/sec. Note that only at the 0 yaw condition is the angle independent of the rotation cycle.

Another significant geometry effect is driven by the wind velocity deficit experienced by the blade as it passes through the flow wake behind the cylindrical support tower. This tower shadow effect creates a momentum deficit which impacts the blade when it rotates behind the cylindrical support (180 deg). The rapid change of inlet velocity in this region reduces the local angle of attack along the span of the blade. This characteristic is prevalent with any down wind turbine and creates a periodic perturbation to the blade during each and every rotation cycle. It should be noted that for this down wind test geometry, there can be no truly steady state flow condition throughout any rotation cycle. As a minimum, the aerodynamics of the blade will always be affected by the tower wake. Also, as seen in Fig. 5, the effect of tower shadow is additive to the yaw effect and varies with changes in the inlet velocity vector. The location of the shadow / blade impact zone also varies with changes in the relative yaw angle.

The relations described above show that the angle of attack for a blade can and will vary widely for different inflow characteristics as well as for geometric structural interactions with the support tower and other turbine elements. At any given time the aerodynamic forces over the blades can vary by more than a factor of ten at specific chord locations and at different span locations.

Turning to the data available from the Combined Experiment, the wind velocity and angle averages were obtained for each 5 min test episode; these are shown in Fig. 6. Clearly, most of the available data were collected at modest velocities and angles. However, the high variance values suggest that within each 5 min data taking episode there may have been wide variations in these inflow conditions. As shown above, such conditions would severely limit the usefulness of using aerodynamic averages based upon inflow averages.

Combined Experiment Data Distribution
Mean Velocity and Standard Deviation

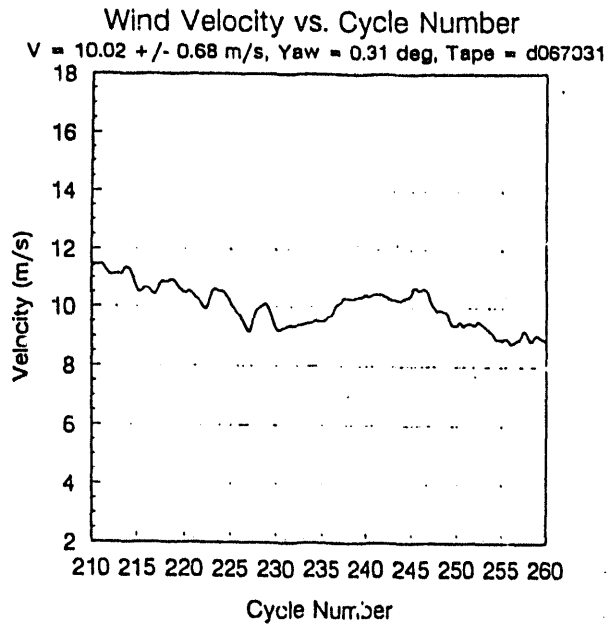
		Average Velocity (m/s)						Run Ave.
		<5	5-8	8-11	11-14	14-17	>17	
Average Yaw (degrees)	-15--9	-	7.4 ± 1.7	10.3 ± 3.0	-	-	-	8.3 ± 2.5
	-9--3	4.2 ± 1.4	6.4 ± 1.5	9.2 ± 1.9	12.8 ± 2.9	14.8 ± 2.8	17.8 ± 3.2	11.4 ± 4.7
	-3--3	4.7 ± 1.5	7.3 ± 1.3	9.3 ± 1.6	12.4 ± 2.6	15.5 ± 2.8	-	9.5 ± 3.6
	3--9	-	6.8 ± 1.5	-	-	14.2 ± 3.7	-	8.3 ± 3.6
	9--15	-	7.7 ± 1.4	-	-	-	-	7.7 ± 1.4
	Column Averages		4.6 ± 1.5	7.0 ± 1.3	9.3 ± 1.8	12.6 ± 2.8	15.0 ± 2.9	17.8 ± 3.2
		Total						

Combined Experiment Data Distribution
Mean Yaw and Standard Deviation

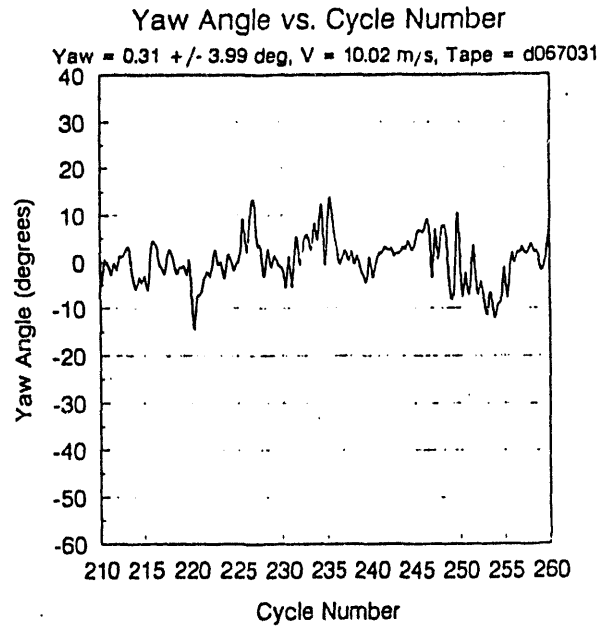
		Average Velocity (m/s)						Run Ave.
		<5	5-8	8-11	11-14	14-17	>17	
Average Yaw (degrees)	-15--9	-	-15.4 ± 15.3	-9.4 ± 21.3	-	-	-	-13.5 ± 17.6
	-9--3	-9.1 ± 20.1	-5.3 ± 14.4	-4.6 ± 11.8	-4.6 ± 18.9	-4.3 ± 11.6	-3.6 ± 12.7	-4.7 ± 12.7
	-3--3	-0.3 ± 9.7	0.0 ± 11.3	-1.3 ± 11.6	-1.1 ± 12.9	-2.1 ± 11.9	-	-0.9 ± 11.6
	3--9	-	3.8 ± 12.6	-	-	5.6 ± 13.7	-	4.1 ± 12.8
	9--15	-	13.5 ± 20.9	-	-	-	-	13.5 ± 20.9
	Column Averages		-2.9 ± 14.6	-1.4 ± 14.6	-3.0 ± 12.7	-3.2 ± 11.8	-2.3 ± 12.4	-3.6 ± 12.7
		Total						

To evaluate the velocity and angle changes within the 5 minute episodes, all episodes were broken down into average velocity and angle characteristics for each individual cycle. It immediately became clear that the averages were not good indications of inflow velocities and angles suitable for aerodynamic analyses. For example, the plots of Fig. 7, show the consecutive time histories of velocity and angle for two test episodes that have approximately the same average values. Across the two episodes both velocity and angle changes are rapid and large. Clearly, these changes were extremely large in one episode. But, both episodes contained sufficient variability to prevent a meaningful aerodynamic analysis of the aerodynamics of the wind turbine. The local angles of attack were clearly varying widely yielding different aerodynamic performance and they were varying rapidly enough to signal the opportunity for dynamic stall events.

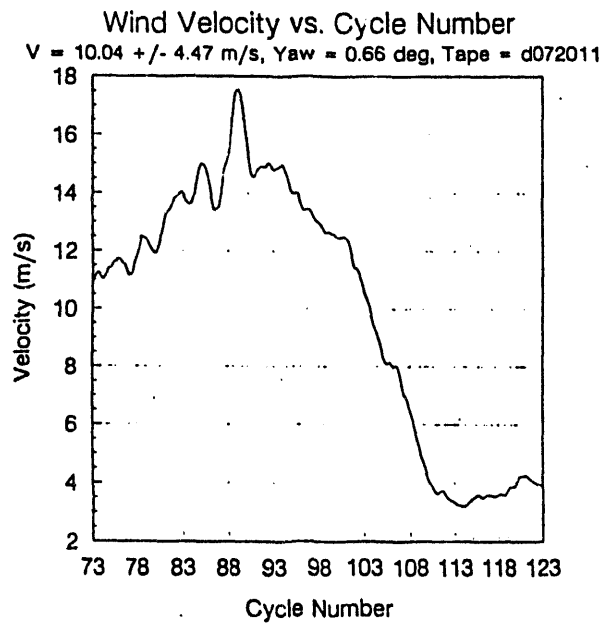
FIGURE 6: DISTRIBUTION OF INFLOW DATA FOR ALL FIVE MINUTE TEST EPISODES. MEANS AND STANDARD DEVIATIONS ARE GIVEN FOR FREESTREAM VELOCITY IN THE TOP CHART AND YAW IN THE BOTTOM CHART.



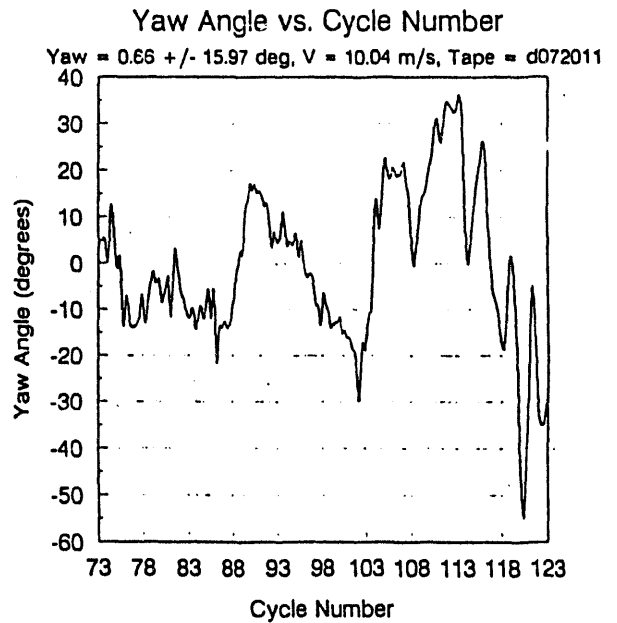
A)



B)



C)



D)

FIGURE 7: FIFTY CONSECUTIVE CYCLE TIME HISTORIES IN VELOCITY AND YAW FOR TWO EPISODES HAVING APPROXIMATELY THE SAME MEAN VALUES. BOTH EPISODES SHOW LARGE, RAPID CHANGES IN BOTH VELOCITY AND YAW. A) AND B) ILLUSTRATE THE VELOCITY AND YAW, RESPECTIVELY, FOR RELATIVELY CALM INFLOW CONDITIONS. C) AND D) ARE THE INFLOW CONDITIONS FOR A FAR MORE VARIABLE EPISODE.

To enable an aerodynamic analysis of the turbine it was necessary to limit inflow variance. Thus, the whole data set was scanned for those instances where inflow velocities and angles were well behaved. Two approaches were employed. First, data were obtained for instances where at least 3 consecutive cycles exhibited approximately the same velocities at approximately zero yaw angles. Using this approach, less than 1% of the data could be used as indicative of relatively steady inflow conditions. However, we had data from cycles where the inflow was nearly as well controlled as it is in wind tunnel testing. And, these data covered a fair range of test velocities. The second approach identified 50 consecutive cycles of data where the inflow conditions were relatively well-behaved. Here, the rationale was that the integrated pressure measurements should be about the same for similar inflow conditions. Thus, correlations of the pressure histories over the blades should be high for similar inflow conditions across cycles. The cycles with high pressure history cross correlations between each other were identified and the velocities for these cycles were determined. Again, these data sets were selected for near zero yaw conditions.

The results of these two different approaches are co-plotted in Fig. 8, for a range of velocities. The results correlate well, particularly at lower velocities. The highest velocities reveal a particularly interesting facet of turbine blade performance. The most inboard span location shows aerodynamic performance far in excess of that seen at other span locations and that expected from wind tunnel testing. The blade can not be stalled and show such aerodynamic performance. This must represent a very different set of flow-blade interactions than characteristic of the more outboard span locations.

In Fig. 9, these relations are plotted as a function of angle of attack. Also shown in this plot are the performance values of this airfoil blade as tested in the wind tunnel. For low angles of attack, the performance of the blade is exactly as expected from the wind tunnel data and the two approaches coincide with these data. At slightly higher angles, the turbine data exceeds the expected values obtained from the wind tunnel. Interestingly, these are operational regimes where the vector sums of velocities are expected to put the blade into a dynamic stall condition. The high transient lift of dynamic stall would be expected to provide higher blade aerodynamic loading than observed in the wind tunnel tests.

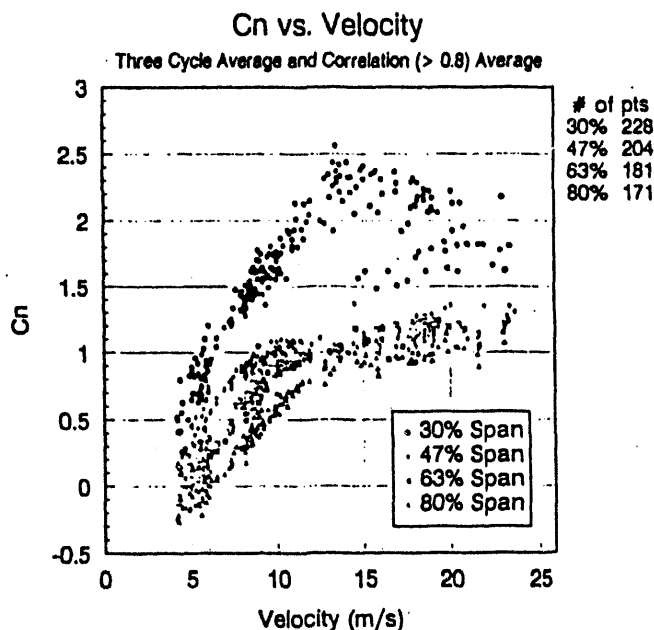


FIGURE 8: COMPARISON OF INDEPENDENT APPROACHES FOR C_N VERSUS VELOCITY SHOWING CONSISTENCY OF THE RESULTS.

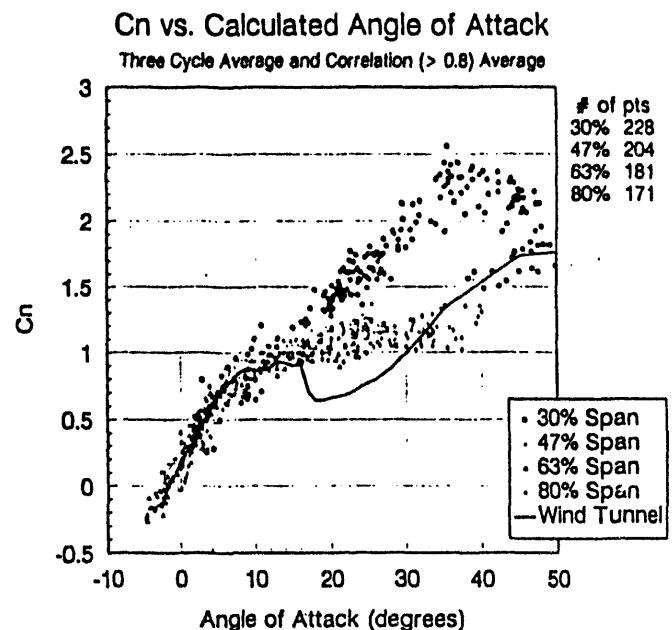


FIGURE 9: COMPARISON OF INDEPENDENT APPROACHES TO WIND TUNNEL DATA ILLUSTRATING THE DIFFERENT OPERATIONAL REGIMES.

The inboard span location anomaly in performance is even more obvious using this analysis. The angle of attack for 30% span must be inaccurate either due to geometry altered flow velocities or to geometry driven changes in crossflow. Nevertheless, the analysis has now clearly identified those operational regimes that constitute aerodynamic problems for the wind turbine. These operational regimes were co-mingled in previous studies using average values.

To begin to use these clearly identified regimes to understand the nature of aerodynamic difficulties experienced by wind turbines, several anomalous performance cycles were identified and evaluated in detail. The pressure histories (Fig. 10) for 30% span locations are shown for relatively high velocities and for high yaw angles. It is clear that when the vector sum of wind velocity, rotational velocity and yaw angle produce a rapid change in angles of attack a brief dynamic stall event occurs with the signature of a high pressure transient. This is particularly evident with the lower wind velocity experienced in the tower wake. In other instances, a high crossflow condition exists wherein a less transient, high pressure plateau is produced in the pressure profile. These are but two graphic examples of previously unpredicted aerodynamic loading events that are certain to be difficult for the wind turbine to handle.

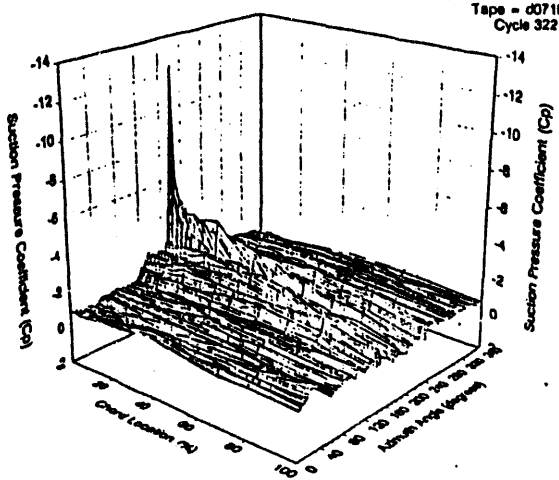
Being able to identify these aerodynamic events makes it possible to do correlations with mechanical loading time histories and with power generation time histories. Taken together, these data promise to provide a more rational basis for both wind turbine design and operation protocols.

REFERENCES

Butterfield, C.P., W.P. Musial, and D.A. Simms, 1992, Combined Experiment Phase I Final Report, TP-257-4655, NREL, Golden, CO.

Huyer, S.A., 1992, Examination of Forced Unsteady Separated Flow Fields on a Rotating Wind Turbine Blade, TP-442-4864, NREL, Golden, CO.

One Cycle Upper Surface Pressure Distribution
30% Span Location



One Cycle Upper Surface Pressure Distribution
30% Span Location

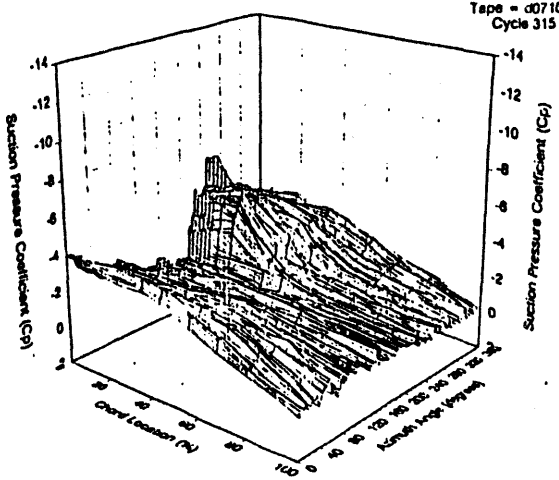


FIGURE 10: PRESSURE HISTORIES AT 30% SPAN FROM TWO ANOMALOUS AERODYNAMIC EVENTS. THE PROFILE ON THE LEFT SHOWS A HIGH TRANSIENT PEAK INDICATIVE OF A DYNAMIC STALL EVENT. THE PROFILE ON THE RIGHT SHOWS A HIGH PRESSURE PLATEAU.